

## Preparation of Poly(7-formylindole)/carbon Fibers Nanocomposites and Their High Capacitance Behaviors

Guo Ye<sup>1,§</sup>, Xiumei Ma<sup>2,§</sup>, Yun He<sup>2</sup>, Xuemin Duan<sup>1</sup>, Weiqiang Zhou<sup>2,\*</sup>, Jingkun Xu<sup>1,\*</sup>

<sup>1</sup> School of Pharmacy, Jiangxi Science and Technology Normal University, Nanchang 330013, China

<sup>2</sup> Jiangxi Engineering Laboratory of Waterborne Coatings, Jiangxi Science and Technology Normal University, Nanchang 330013

\*E-mail: [zhouwqh@163.com](mailto:zhouwqh@163.com), [xujingkun@jxstnu.edu.cn](mailto:xujingkun@jxstnu.edu.cn)

§Guo Ye and Xiumei Ma, these authors contributed equally to this work.

Received: 16 May 2017 / Accepted: 25 July 2017 / Published: 13 August 2017

Polyindoles belonging to the fused-ring family have attracted extensive investigation as promising materials due to their unique physical and electrochemical properties. Herein, poly(7-formylindole) (PFIIn) film was firstly synthesized electrochemically on carbon fibers by direct anodic oxidation of 7-formylindole in acetonitrile solution containing 0.1 M LiClO<sub>4</sub>. FT-IR spectra indicated that the polymerization site of monomer happened at the C<sub>2</sub> and C<sub>3</sub> positions of indole ring. The morphology of PFIIn film on carbon fibers was investigated through SEM observation, which indicated that PFIIn film tightly wrapped over carbon fibers (PFIIn/CF). Electrochemical results indicated that PFIIn/CF electrode showed a remarkable specific capacitance of 637 F g<sup>-1</sup> at 20 A g<sup>-1</sup>. The energy density reached about 42 Wh kg<sup>-1</sup> at a high power density of 21 kW kg<sup>-1</sup>. Furthermore, PFIIn/CF still maintained about 74.1% of initial specific capacitance and 100% coulombic efficiency after 1000 cycles. These results revealed that PFIIn/CF was a promising electrode material for the flexible supercapacitors application.

**Keywords:** Supercapacitors; Conducting polymer; Poly(7-formylindole); Carbon fibers; Capacitance performance

### 1. INTRODUCTION

Supercapacitors as new energy storage devices have attracted intense attention due to their distinguishing features such as fast charge-discharge rates, high power density and long cycle life [1,2]. Nowadays, supercapacitors have been widely employed in consumer electronics, industrial power and intelligent start-stop system [3,4]. In order to further advance the performance of

supercapacitors, the improvement in performance of electrode materials is one of the most critical factors. Electrode materials mainly include carbon-based materials, metal oxide and conducting polymers, in which carbon-based materials produce capacitance by pure electrostatic charges accumulation at the electrode/electrolyte interface [5], whereas the capacitance of metal oxides and conducting polymers (CPs) arises from their redox or Faradaic charge reactions taking place on the surface of the materials [6]. Generally, electrode materials with large specific surface areas possess high capacitance. Therefore, for enhancing the specific surface area, a wide variety of nanostructure materials have been designed [7-11], for instance, nanoions, nanotubes, nanowires, nanoparticles, and nanoflowers.

CPs such as polyaniline, polypyrrole, polythiophene and their derivatives have been studied [12]. They possessed higher specific capacitance and energy density compared to carbon-based materials. However, the limitation of CPs is mainly their lower cycle stability [13]. In order to enhance the cycle stability of CPs, research works focus on the composite construction [14-16], the nanomaterial preparation [17-19], special anionic dopants use [20,21] and the polymer's structure functionalization [22-24]. Polyindole, similar to the aforementioned CPs, possesses combined excellent properties of both poly(*para*-phenylene) and PPy such as fairly good thermal stability [25], highly stable redox activity [26], fast switchable electrochromic ability [26] and air stable electrical conductivity in the doped state [27]. Presently, polyindole and its derivatives and composites as supercapacitors electrode materials have been also reported and showed high cycle stability and specific capacitance [28-34].

Among polyindole derivatives, formyl-substituted polyindole has many unique properties, for example, the electron-withdrawing formyl group substitution can decrease the LUMO level of polymers, diminishing the band gap of polymers [35]; the formyl group can improve the thermal stability of the polymers [36]; the formyl group is strongly reactive towards a variety of nucleophiles [37,38]; in addition, the N-H group on indole unit forms intermolecular hydrogen bonds, inducing the nanowire formation [31]. Therefore, the presence of N-H and formyl groups possibly facilitate to improve the electrochemical behavior of polyindole. Nie *et al.* used conducting poly(5-formylindole) to fabricate the electrochemiluminescence biosensor [39], electrochemical immunosensor [40] and electrochromic device [41]. Above information foreshows that the formyl-substituted polyindole is a new interesting CPs material. For seeking new high capacitive performance materials, it is very necessary to research the capacitive behaviors of formyl-substituted polyindole.

In this paper, poly(7-formylindole) (PFIIn) was electrodeposited on carbon fiber (CF) by direct anodic oxidation of 7-formylindole in acetonitrile/HClO<sub>4</sub> solution and evaluated the capacitive behavior of PFIIn/CF. The novelties about this work are mainly summarized as follows: (1) for 7-formylindole, N-H group on indole unit would form intermolecular hydrogen bonds as well as intramolecular hydrogen bonds with oxygen atoms in the special formyl group on 7 position, which makes for the formation of PFIIn nanowires, (2) the carbon fiber possesses good flexibility, high conductivity, outstanding stability, and 3-D structural feature, which will be advantageous to form a 3-D PFIIn/CF core/shell structure composite [42], (3) poly(7-formylindole) as new capacitive materials has not been reported yet, and (4) 3-D PFIIn/CF has high capacitive performance proved by electrochemical techniques.

## 2. EXPERIMENTAL

### 2.1. Materials

7-Formylindole (FIn) was purchased from Shanghai Vita Chemical Reagent Co., Ltd. China. Carbon fiber cloth (WOS1002, Ce Tech) was supplied by Phychemi Company Limited, China. Lithium perchlorate ( $\text{LiClO}_4$ , AR) was bought from Xiys Reagent Research Center. Acetonitrile (ACN, AR) and  $\text{HClO}_4$  (72%) were provided by Shanghai Lingfeng Chemical Reagent Co., Ltd and used after reflux distillation and Xiya Reagent Research Center, respectively.

### 2.2 Apparatus

A CHI660E potentiostat/galvanostat (Shanghai Chenhua Instrumental Co., Ltd., China) was used to finish the electrochemical experiments. The carbon fiber cloth was used as substrate electrode. The reference electrode with Ag/AgCl and saturated calomel electrode (SCE) were used for electrodeposition and performance testing of polymer, respectively. The counter electrode was platinum wire. For the EIS measurement, the amplitude of modulation potential was 5 mV, and the frequency varied from 15 kHz to 0.01 Hz. ZSimpWin software was used to fit the impedance data.

Bruker Vertex 70 Fourier transform infrared (FT-IR) spectrometer with samples in KBr pellets was used for Infrared spectra measurement. Scanning electron microscope (JSM-5600, JEOL) was employed in the Scanning electron microscope (SEM) measurements.

### 2.3. Preparation of PFIIn

The PFIIn film was prepared potentiostatically on CF substrates ( $0.5 \text{ cm} \times 0.5 \text{ cm}$ ) at 1.0 V in ACN solution containing 100 mM FIn and 0.1 M  $\text{LiClO}_4$ . The mass of PFIIn film (approximately 4.72  $\mu\text{g}$ ) was controlled from the total charge passed through the cell during the film growth process [30]. After the electrodeposition, the prepared PFIIn/CF was washed repeatedly with ACN and double-distilled deionized water to remove the monomer and electrolyte.

### 2.4. Capacitance calculation

In the GCD method, the specific capacitance was calculated by utilizing the formula [43].

$$C = \frac{It}{mV} \quad (1)$$

in which,  $C$  is the specific capacitance ( $\text{F g}^{-1}$ ).  $I$ ,  $t$  and  $m$  are the charge-discharge current (A), the discharge time (s) and the mass of the polymer (g).

In the CV method, the specific capacitance was calculated by means of the equation [44].

$$C = \frac{\int_{E_1}^{E_2} i(E) d(E)}{2vm(E_2 - E_1)} \quad (2)$$

where,  $E_1$  and  $E_2$  are the cut-off potentials in the cycle voltammetry,  $i(E)$  is the instantaneous current.  $\int_{E_1}^{E_2} i(E)d(E)$  the area of CV curve is the total charge.  $v$  and  $m$  is the scan rate ( $\text{mV s}^{-1}$ ) and the mass of the electrochemical polymer (g), respectively.

The energy density ( $E$ , Wh kg) and the power density ( $P$ , W kg) were calculated through the ways [45].

$$E = \frac{1}{2} CV^2 \quad (3)$$

$$P = \frac{E}{\Delta t} \quad (4)$$

where,  $C$  is the specific capacitance.  $V$  and the  $\Delta t$  were the scope of potential and the discharge time, respectively.

### 3. RESULTS AND DISCUSSION

#### 3.1 Cyclic voltammetry of FIn

The successive CVs of FIn monomer on CF were carried out in ACN solution containing 0.1 M  $\text{LiClO}_4$ , as shown in Fig. 1.

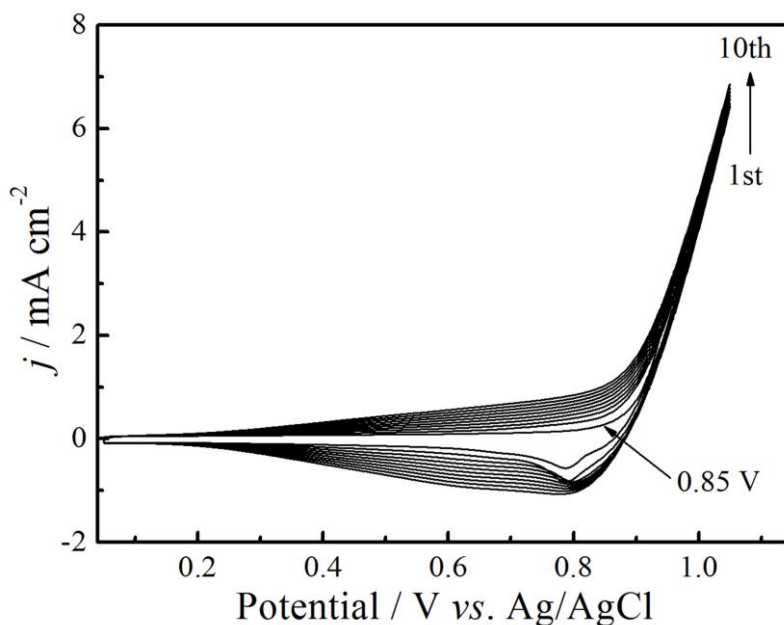


**Figure 1.** CVs of 100 mM FIn on CF in ACN solution containing 0.1 M  $\text{LiClO}_4$  at  $100 \text{ mV s}^{-1}$ .

The CVs of monomer were involved in the two processes, *i.e.* the polymerization of monomers and the redox reaction of as-formed polymer. As seen from the first positive scan, the polymerization of monomer started at about 0.85 V. Over the potential, there was a steep rise in the current density ( $j$ ). This phenomenon came from the formation of a large number of free radical cations and subsequent their polymerization reaction. When the scan was reverse, the reduction of polymer appeared.

However, following CVs showed the oxidation of polymer and monomer in the positive scan, and the reduction of polymer in the negative scan. As the scan proceeded, the  $j$  of broad redox peaks gradually increased, indicating the mass of film increased.

### 3.2 Structure of PFI<sub>n</sub>

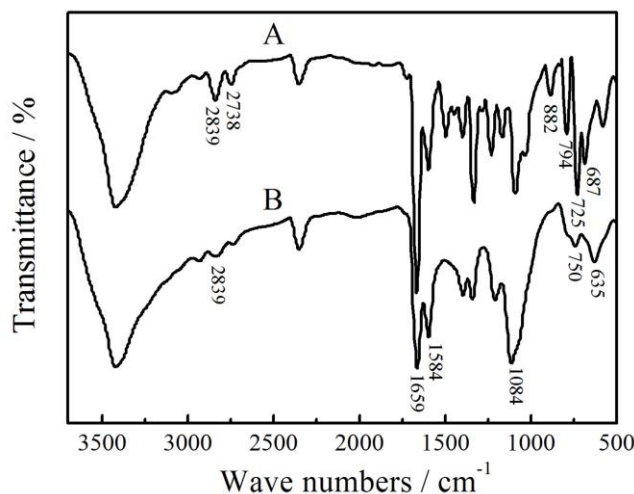


**Figure 2.** FT-IR spectra of FI<sub>n</sub> (A) and PFI<sub>n</sub> (B).

Fig. 2 shows the FT-IR spectra of FI<sub>n</sub> (A) and PFI<sub>n</sub> (B). The several bands at around 2839  $\text{cm}^{-1}$  and at near 1659  $\text{cm}^{-1}$  belong to CH stretching on C(=O)-H and C=O stretching, respectively. This bands at 1584  $\text{cm}^{-1}$  and 3429  $\text{cm}^{-1}$  were attributed to be the deformation and the stretching vibrations of the N-H bond on indole ring, respectively. Above bands all were present in the spectra of monomer and polymer. In the spectrum of PFI<sub>n</sub>, the bands at 1084  $\text{cm}^{-1}$  and 635  $\text{cm}^{-1}$  were the dopant  $\text{ClO}_4^-$  [46], which indicated that PFI<sub>n</sub> was in doped state. In addition, the band at 750  $\text{cm}^{-1}$  in spectrum of PFI<sub>n</sub> was ascribed to C-H deformation vibration of benzene ring (3 adjacent hydrogens), which suggested that benzene ring on PFI<sub>n</sub> unit was 1,2,3-trisubstitution. Hence, the electrochemical polymerization of FI<sub>n</sub> monomer happened at the C<sub>2</sub> and C<sub>3</sub> positions of indole ring.

### 3.3 Morphology of PFI<sub>n</sub>/CF

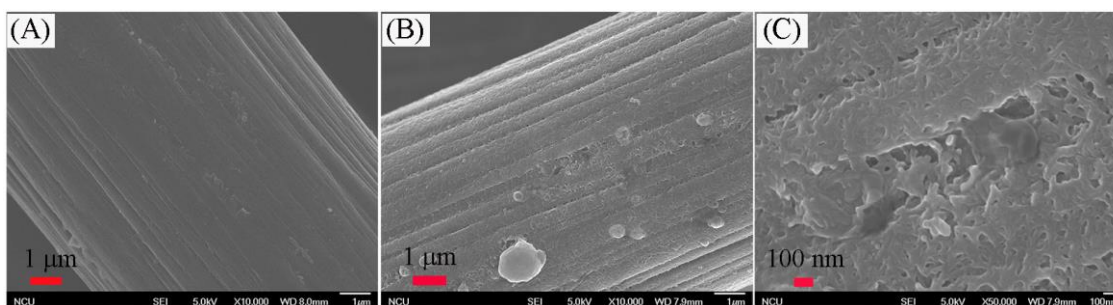


**Figure 3.** SEM of bare CF (A) and PFI<sub>n</sub>/CF (B&C)

Fig. 3 shows the SEM of the bare CF(A) and the PFIIn/CF (B&C). In Fig. 3A, the CF had a smooth surface with about 11  $\mu\text{m}$  diameter. When the polymer film was deposited on the surface of CF, the surface changed to be rough (Fig. 3B). It can be seen from the more microscopic image in Fig. 3C, PFIIn enwrapped tightly the CF, forming a 3-D core/shell structure. PFIIn seemed to be flat network composed of nanowires. The network structure will facilitate to improve the specific capacitance of electrode.

### 3.4 Capacitive behaviors of PFIIn/CF

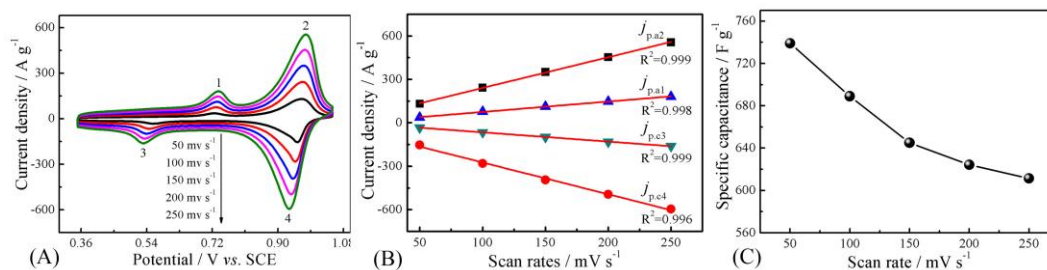


**Figure 4.** (A) CVs of PFIIn/CF electrode in 0.1 M HClO<sub>4</sub> at the different scan rates, and (B) peak current densities as a function of scan rates, and (C) the specific capacitance as a function of scan rate.

The CVs of the PFIIn/CF electrode were studied in 0.1 M HClO<sub>4</sub> solution at different scan rates, as shown in Fig. 4A. The CV shape of PFIIn/CF electrode at high potential, namely a pair of redox peaks at around 0.9 V, this process involved not only electronic exchanges but also the effect of pH, so that resulted in the increased current densities and sharp redox peaks [30], which was similar to those of poly(indole-carboxylic acid) [31], poly(5-formylindole)[39], poly(5-nitroindole) [47] and poly(5-cyanoindole) [48]. Additionally, the current density of redox peaks increased linearly as the scan rate increased from 50 to 250 mV s<sup>-1</sup> (Fig. 4B) The difference was the reduction at 0.5 V and oxidation peaks at 0.7 V were very well-defined. This should be due to the electronic exchanges that caused by the reaction of formyl group on indole ring and this process was pH independent [31]., which implied that the electrochemical process of PFIIn/CF electrode was an adsorption controlled process. The plot about the specific capacitance of PFIIn/CF electrode as a function of scan rates reflects distinctly that the specific capacitance decreased with the increase of scan rates (Fig. 4C). The calculated specific capacitance was 739 F g<sup>-1</sup> at 50 mV s<sup>-1</sup> and then decreased to 611.4 F g<sup>-1</sup> at 250 mV s<sup>-1</sup>, with a decrease of about 17.3%. The high specific capacitance at high scan rates shows that PFIIn/CF electrode is a potential electrode material for supercapacitors.

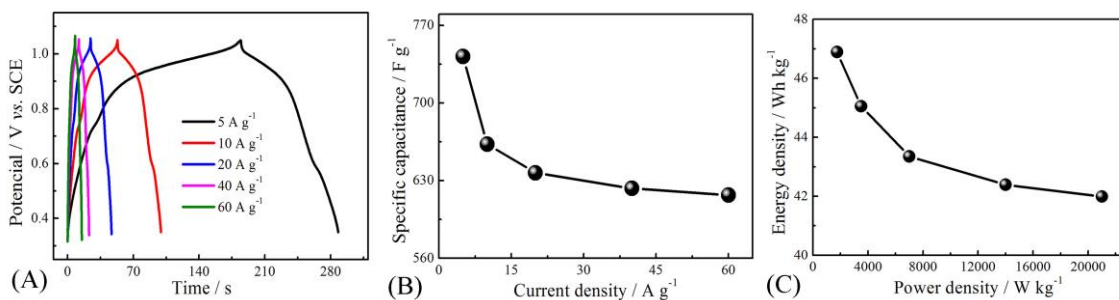


**Figure 5.** GCD curves of PFIIn/CF (A) in 0.1 M HClO<sub>4</sub> solution at different current density, (B) Specific capacitance of PFIIn/CF as a function of current density, and (C) Ragone plots of PFIIn/CF electrode.

The GCD of PFIIn/CF electrode was conducted at different current densities and potential window of 0.7 V. As seen from the Fig. 5A, the charge-discharge curves deviated from the triangle shape, which was caused by the redox reaction of PFIIn. At different current density, the charge-discharge curves are similar. When the current densities were 5 A g<sup>-1</sup>, 10 A g<sup>-1</sup>, 20 A g<sup>-1</sup>, 40 A g<sup>-1</sup> and 60 A g<sup>-1</sup>, the corresponding specific capacitances were 742 F g<sup>-1</sup>, 662 F g<sup>-1</sup>, 637 F g<sup>-1</sup>, 622 F g<sup>-1</sup> and 617 F g<sup>-1</sup> (Fig. 5B). The specific capacitance of PFIIn/CF electrode at 60 A g<sup>-1</sup> still remained approximately 82.2% of specific capacitance at 5 A g<sup>-1</sup>. This indicated that PFIIn/CF electrode had high rate capability. In addition, in Fig. 5C, the energy density was 46.9 Wh kg<sup>-1</sup> at the power density of 1750 W kg<sup>-1</sup>, and more importantly, the energy density still reached 42 Wh kg<sup>-1</sup> at the high power density of 21000 W kg<sup>-1</sup>.

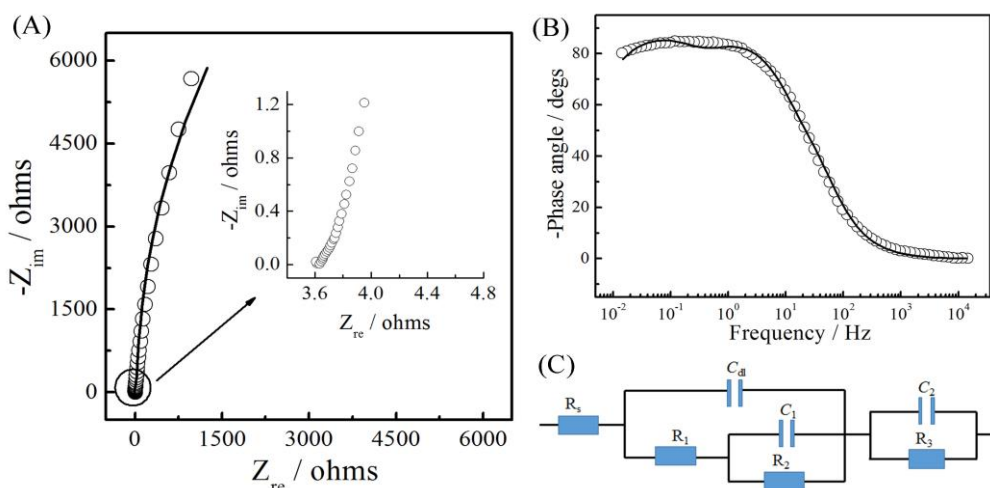


**Figure 6.** Nyquist plots (A) and Bode-phase angle plots (B) of PFIIn/CF in 0.1 M HClO<sub>4</sub> solution and the corresponding calculated results (fitting line) based on the equivalent circuit (C).

The capacitive behaviors of PFIIn/CF was also studied by EIS technology. Fig. 6 shows the EIS of PFIIn/CF in 0.1 M HClO<sub>4</sub> solution. At the low frequency, the PFIIn/CF electrode showed almost vertical curve, which indicated PFIIn/CF had a good capacitor behavior (Fig. 6A). In the high frequency region, a very small semicircle can be seen for the PFIIn/CF electrode (Fig. 6A, inset),

suggesting a rapid electronic and ionic transfer [48]. At about 0.01 Hz, the phase angles reached  $-80^\circ$  (Fig. 6B). On the basis of the above measured impedance, an equivalent circuit model was proposed in Fig. 6C. According to the proposed equivalent circuit model, the chi-squared ( $\chi^2$ ) defined as the sum of the squares of the residuals reached  $9.38 \times 10^{-4}$ , which indicated that the simulation calculated results were well in accordance with the measured results [49]. In the equivalent circuit model,  $R_s$  ( $3.76 \text{ ohm cm}^{-2}$ ) is the solution resistance;  $C_{dl}$  ( $1.2 \text{ mF cm}^{-2}$ ) shows the double layer capacitance;  $R_1$  ( $15.32 \text{ ohm cm}^{-2}$ ) is the resistance of PFIIn film;  $R_2$  ( $3.0 \times 10^4 \text{ ohm cm}^{-2}$ ) is the charge transfer resistance at the polymer/solution interface;  $C_1$  ( $0.6 \text{ F cm}^{-2}$ ) is the pseudocapacitance of PFIIn film;  $C_2$  ( $7.9 \text{ mF cm}^{-2}$ ) and  $R_3$  ( $54.13 \text{ ohm cm}^{-2}$ ) are the capacitance and the resistance of the CF substrate, respectively. From the corresponding fitting parameters provided in Table 1, it can be seen that the double layer capacitance is much smaller than the pseudocapacitance of PFIIn, and  $C_2$  value is very small compared to system's overall capacitance.

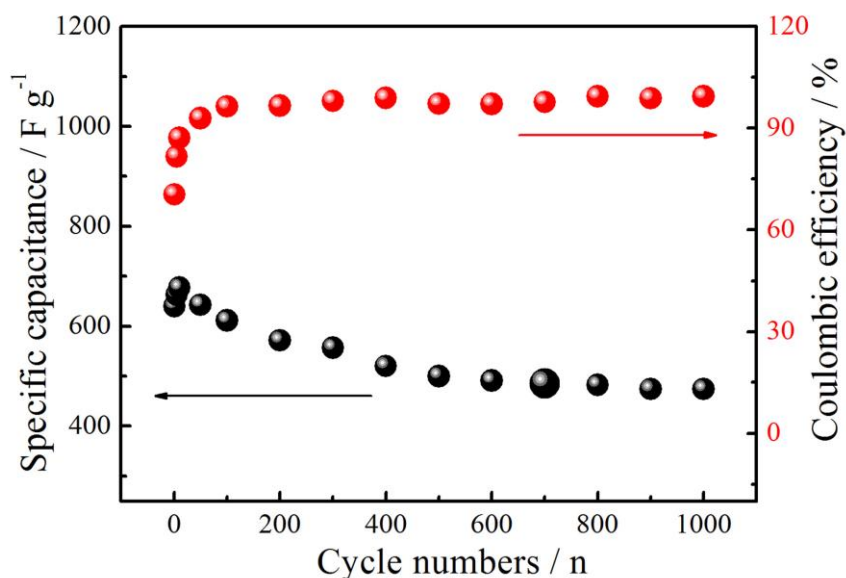


**Figure 7.** Cycle stability and the coulombic efficiency of PFIIn/CF electrode at  $20 \text{ A g}^{-1}$ .

Cycle stability and the coulombic efficiency of electrode for supercapacitors are very important. Fig. 7 shows the cycle life and the coulombic efficiency of PFIIn/CF electrode at  $20 \text{ A g}^{-1}$ . As seen from Fig. 7, the specific capacitance gradually increased at initial 10 cycles, and then started to decrease slowly. After 600 cycles, it tended to be stable. Moreover, the coulombic efficiency and the specific capacitance still maintained about 100% and 74.1% after 1000 cycles, respectively. This indicated PFIIn/CF electrode had a high cycle life.

#### 4. CONCLUSIONS

In this paper, PFIIn was successfully electrodeposited on CF by direct anodic oxidation of FIIn monomer in acetonitrile/ $\text{HClO}_4$  solution, forming a 3-D PFIIn/CF core/shell structure composite electrode. The electrochemical polymerization of FIIn monomer happens at the  $C_2$  and  $C_3$  positions of

indole ring. The specific capacitance of PFIIn/CF electrode reached  $637 \text{ F g}^{-1}$  at  $20 \text{ A g}^{-1}$ , and its energy density was about  $42 \text{ Wh kg}^{-1}$  at a high power density of  $21 \text{ kW kg}^{-1}$ . Furthermore, PFIIn/CF electrode showed a higher cycle stability, *i.e.* about 74.1% of initial specific capacitance after 1000 cycles. This implied that PFIIn/CF was a promising electrode material for the supercapacitors.

#### ACKNOWLEDGEMENT

This work was supported by the National Natural Science Foundation of China (grant number: 51662012, 51572117), the Natural Science Foundation of Jiangxi Province (20161BAB206147), the Jiangxi Provincial Department of Education (GJJ160762), Young top-notch talent (2016QNBjRC001) of Jiangxi Science and Technology Normal University.

#### References

1. M. Winter, R. Brodd, *Chem. Rev.*, 104 (2004) 4245.
2. Y. Shao, M. El-Kady, L. Wang, Q. Zhang, Y. Li, H. Wang, M. Mousavi, R. Kaner, *Chem. Soc. Rev.*, 44 (2015) 3639.
3. E. Karden, S. Ploumen, B. Fricke, T. Miller, K. Snyder, *J. Power Sources*, 168 (2007) 2.
4. J. Yeo, G. Kim, S. Hong, M. Kim, D. Kim, J. Lee, H. Lee, J. Kwon, Y. Suh, H. Kang, *J. Power Sources*, 246 (2014) 562.
5. A. Pandolfo, A. Hollenkamp, *J. power sources*, 157 (2006) 27.
6. G. Wang, L. Zhang, J. Zhang, *Chem. Soc. Rev.*, 41 (2012) 797.
7. C. Hu, K. Chang, M. Lin, Y. Wu, *Nano Lett.*, 6 (2006) 2690.
8. V. Muniraj, C. Kamaja, M. Shelke, *ACS Sustain Chem. Eng.*, 4 (2016) 2528.
9. R. Patil, C. Chang, R. Devan, Y. Liou, Y. Ma, *ACS Appl. Mater. Inter.*, 8 (2016) 9872.
10. Y. Zhu, Y. Wang, Y. Shi, J. Wong, H. Yang, *Nano Energy* 3 (2014) 46.
11. D. Pech, M. Brunet, H. Durou, P. Huang, V. Mochalin, Y. Gogotsi, P. Taberna, P. Simon, *Nature Nanotech.*, 5 (2010) 651.
12. G. Snook, P. Kao, A. Best, *J. Power Sources*, 196 (2011) 1.
13. Y. Song, T. Liu, X. Xu, D. Feng, Y. Li, X. Liu, *Adv. Funct. Mater.*, 25 (2015) 4626.
14. H. Cong, X. Ren, P. Wang, S. Yu, *Energ. Environ. Sci.*, 6 (2013) 1185.
15. Q. Zhang, Y. Li, Y. Feng, W. Feng, *Electrochim. Acta*, 90 (2013) 95.
16. H. Tang, J. Wang, H. Yin, H. Zhao, D. Wang, Z. Tang, *Adv. Mater.*, 27 (2015) 1117.
17. Y. Huang, M. Zhu, Z. Pei, Y. Huang, H. Geng, C. Zhi, *ACS Appl. Mater. Inter.*, 8 (2016) 2435.
18. H. Mi, J. Zhou, Z. Zhao, C. Yu, X. Wang, J. Qiu, *RSC Adv.*, 5 (2015) 1016.
19. R. Liu, S. Cho, S. Lee, *Nanotechnology* 19 (2008) 215710.
20. K. Shi, I. Zhitomirsky, *J. Power Sources*, 240 (2013) 42.
21. S. Chen, I. Zhitomirsky, *J. Power Sources*, 243 (2013) 865.
22. D. Yiğit, T. Güngör, M. Güllü, *Org. Electron.*, 14 (2013) 3249.
23. M. Güllü, D. Yiğit, *Synthetic Met.*, 162 (2012) 1434.
24. E. Ermiş, D. Yiğit, M. Güllü, *Electrochim. Acta*, 90 (2013) 623.
25. P. Abthagir, K. Dhanalakshmi, R. Saraswathi, *Synthetic Met.*, 93 (1998) 1.
26. E. Maarouf, D. Billaud, E. Hannecart, *Mater. Res. Bull.*, 29 (1994) 637.
27. D. Billaud, E. Maarouf, E. Hannecart, *Synthetic Met.*, 69 (1995) 571.
28. R. Raj, P. Ragupathy, S. Mohan, *J. Mater. Chem., A*, 3 (2015) 24338.
29. X. Zhou, A. Wang, Y. Pan, C. Yu, Y. Zou, Y. Zhou, Q. Chen, S. Wu, *J. Mater. Chem. A*, 3 (2015) 13011.
30. X. Ma, W. Zhou, D. Mo, B. Lu, F. Jiang, J. Xu, *RSC Adv.*, 5 (2015) 3215.

31. X. Ma, W. Zhou, D. Mo, J. Hou, J. Xu, *Electrochim. Acta*, 176 (2015) 1302.
32. Q. Zhou, D. Zhu, X. Ma, J. Xu, W. Zhou, F. Zhao, *RSC Adv.*, 6 (2016) 29840.
33. X. Zhou, Q. Chen, A. Wang, J. Xu, S. Wu, J. Shen, *ACS Appl. Mater. Inter.*, 8 (2016) 3776.
34. W. Zhou, X. Ma, F. Jiang, D. Zhu, J. Xu, B. Lu, C. Liu, *Electrochim. Acta*, 138 (2014) 270.
35. H. Van Mullekom, J. Vekemans, E. Havinga, E. Meijer, *Mat. Sci. Eng. R.*, 32 (2001) 1.
36. M. Guiver, H. Zhang, G. Robertson, Y. Dai, *J. Polym. Sci. Pol. Chem.*, 39 (2001) 675.
37. M. Yaseen, M. Ali, M. NajeebUllah, M. Ali Munawar, I. Khokhar, *J. Heterocyclic Chem.*, 46 (2009) 251.
38. G. Guirado, C. Coudret, M. Hliwa, J. Launay, *J. Phys. Chem. B*, 109 (2005) 17445.
39. G. Nie, Z. Bai, W. Yu, J. Chen, *Biomacromolecules*, 14 (2013) 834.
40. L. Zhang, C. Li, D. Zhao, T. Wu, G. Nie, *Microchim. Acta*, 181 (2014) 1601.
41. G. Nie, L. Zhou, H. Yang, *J. Mater. Chem.*, 21 (2011) 13873.
42. Y. Chen, Y. Hsu, Y. Lin, Y. Lin, Y. Horng, L. Chen, K. Chen, *Electrochim. Acta*, 56 (2011) 7124.
43. M. Stoller, R. Ruoff, *Energ. Environ. Sci.*, 3 (2010) 1294.
44. M. Plonska-Brzezinska, M. Lewandowski, M. Błaszcyk, A. Molina-Ontoria, T. Luciński, L. Echegoyen, *ChemPhysChem*, 13 (2012) 4134.
45. H. Wu, H. Pang, X. Lou, *Energ. Environ. Sci.*, 6 (2013) 3619.
46. H. Talbi, J. Ghanbaja, D. Billaud, B. Humbert, *Polymer*, 38 (1997) 2099.
47. W. Zhou, Y. Du, H. Zhang, J. Xu, P. Yang, (2010). *Electrochim. Acta*, 55 (2010) 2911
48. W. Zhou, D. Huang, X. Ma, J. Xu, F. Jiang, B. Lu, D. Zhu, *Adv. Mater. Research*, 1053 (2014) 235.
49. D. Aradilla, F. Estrany, C. Alemán, *J. Phys. Chem. C*, 115 (2011) 8430.
50. F. Cebeci, H. Geyik, E. Sezer, A. Sarac, *J. Electroanal. Chem.*, 610 (2007) 113.

© 2017 The Authors. Published by ESG ([www.electrochemsci.org](http://www.electrochemsci.org)). This article is an open access article distributed under the terms and conditions of the Creative Commons Attribution license (<http://creativecommons.org/licenses/by/4.0/>).